Long non-coding RNA MBI-52 inhibits the development of liver fibrosis by regulating the microRNA-466g/SMAD4 signaling pathway

YAZHOU LI[1], PEIXIAO LIU[2] and FEIPENG WEI[3]

[1]Department of Pain Intervention, Baoji High-tech People's Hospital, Baoji, Shaanxi 721000; [2]Department of Cardiopulmonary Rehabilitation, Xi'an International Medical Center Hospital, Xi'an, Shaanxi 710000; [3]Department of Interventional Radiology, Tangdu Hospital, Air Force Military Medical University, Xi'an, Shaanxi 710038, P.R. China

Received December 9, 2020; Accepted June 30, 2021

DOI: 10.3892/mmr.2021.12549

Abstract. Liver fibrosis is a wound healing response triggered by liver injury. In severe cases, it may develop into liver cirrhosis, liver cancer and liver failure. Long non-coding RNAs (lncRNAs) play key roles in the development of liver fibrosis. The present study aimed to investigate the role of lncRNA-MBI-52 (lnc-MBI-52) in the progression of liver fibrosis. Carbon tetrachloride (CCl_4)-induced injury was performed to establish a mouse liver fibrosis model, and exogenous transforming growth factor-β1 was used to establish a hepatic stellate cell (HSC) activation model. Reverse transcription-quantitative PCR and western blot analyses were performed to detect mRNA and protein expression, respectively. RNA pull-down assay was performed to assess the interaction between microRNA (miR)-466g and lnc-MBI-52 or SMAD4. Dual-luciferase reporter assay was performed to verify the target of miR-466g. lnc-MBI-52 was overexpressed in CCl_4-induced mouse liver fibrosis models and activated HSCs. lnc-MBI-52 knockdown suppressed liver fibrosis *in vitro*. Moreover, knockdown of lnc-MBI-52 downregulated α-smooth muscle actin and collagen type I expression. In addition, lnc-MBI-52 and SMAD4 were identified as targets of miR-466g. The effects of lnc-MBI-52 on HSC activation were reversed following transfection with miR-466g mimics or SMAD4 knockdown. lnc-MBI-52 miR-466g significantly decreased lnc-MBI-52 expression, while overexpression of lnc-MBI-52 suppressed miR-466g expression. The results of the RNA pull-down assay confirmed the interaction between miR-466g and lnc-MBI-52. Taken together, lnc-MBI-52 induced liver fibrosis by regulating the miR-466g/SMAD4 axis, which may provide a new possible strategy for liver fibrosis.

Correspondence to: Dr Feipeng Wei, Department of Interventional Radiology, Tangdu Hospital, Air Force Military Medical University, 1 Xinsi Road, Baqiao, Xi'an, Shaanxi 710038, P.R. China
E-mail: dr.weifeipeng@hotmail.com

Key words: liver fibrosis, transforming growth factor-β1, long non-coding RNA-MBI-52, microRNA-466g, SMAD4

Introduction

Liver fibrosis refers to the abnormal proliferation of intrahepatic fibrous connective tissue caused by several liver injury factors, which induce an imbalance between the generation and degradation of the extracellular matrix in liver and may progress to liver cirrhosis and liver failure (1-3). Early liver fibrosis may be reversible; thus, identifying the key factors involved in the occurrence of liver fibrosis and understanding the molecular mechanism are crucial for its treatment (4).

Previous studies have demonstrated that long non-coding (lnc)RNAs are involved in a wide range of biological processes and regulate gene expression at multiple levels (5-7). Thus, investigating the molecular mechanisms and role of lncRNAs in liver fibrosis may provide novel therapeutic approaches for its clinical prevention and treatment. lncRNAs are transcribed RNA molecules with a length of >200 nucleotides that have no capacity of protein coding (8). Previous studies have demonstrated that lncRNAs regulate important biological processes, including cell proliferation, survival, apoptosis and differentiation (8-10). Numerous lncRNAs are associated with liver fibrosis (11-13). For example, lnc-MALAT1 can reverse liver fibrosis and the activation of hepatic stellate cells (HSCs) (14). A previous study revealed that the upregulation of lncRNA ENSMUST00000158992 [lncRNA-MBI-52 (lnc-MBI-52)] could promote the progression of liver fibrosis in a mouse model (15). However, the roles of lncRNA ENSMUST00000158992 in human liver fibrosis have not yet been investigated.

MicroRNAs (miRNAs/miRs) are a family of small RNAs that play crucial roles in the occurrence of and protection from liver fibrosis (16). For example, Lan *et al* (17) demonstrated that the process of liver fibrosis is inhibited by upregulating miR-19b-3p and downregulating C-C chemokine receptor type 2 expression. Similarly, miR-181-5p can activate autophagy by modifying the exosomes of adipose-derived mesenchymal

stem cells, thereby preventing liver fibrosis (18). In addition, miR-34a-5p inhibits liver fibrosis by downregulating SMAD4 (19). However, the molecular mechanism underlying the role of miR-466g in liver fibrosis remains unclear.

The present study was undertaken to investigate the roles of lnc-MBI-52 in liver fibrosis using both *in vivo* and *in vitro* assays. The expression levels of mRNAs and miRNAs were detected using reverse transcription-quantitative PCR (RT-qPCR). The expression levels of proteins were determined using western blotting. The interaction between miR-466g and lnc-MBI-52/SMAD4 was verified using dual luciferase reporter and RNA pull-down assays. Cellular functions were detected using a Cell Counting Kit-8 (CCK-8) assay.

Materials and methods

Cell culture and transfection. The human HSC line, LX-2, was purchased from MilliporeSigma (Merck KGaA). Cells were maintained in DMEM (Gibco; Thermo Fisher Scientific, Inc.) supplemented with 10% fetal bovine serum (Gibco; Thermo Fisher Scientific, Inc.), 100 U/ml penicillin and 100 μg/ml streptomycin, at 37˚C in 5% CO_2. TGF-β1 (5 ng/ml; PeproTech, Inc.) was used to induce LX-2 cells and cultured 24 h before transfection.

lnc-MBI-52 small interfering RNA (si-lnc-MBI-52) and scrambled si-Control [si-negative control (NC)], were synthesized by Shanghai GenePharma Co., Ltd. HSCs (6x10^5 cells) were transfected with si-lnc-MBI-52 1# (5'-GCAGAACCA TAAAGATGGTCCA-3'), si-lnc-MBI-52 2# (5'-UGGUAA UGGUGGAGGAAGAUU-3'), si-NC (5'-UUCUCCGAACGU GUCACGUTT-3'), lnc-MBI-52 overexpression (lnc-MBI-52) plasmids (lnc-MBI-52), pcDNA3.1 (vector) (5'-UCACAACCU CCUAGAAAGAGUAGA-3'), miR-466g mimic (5'-UAUGUG UGUGUACAUGUACAUA-3'), mimic NC (5'-UUCUCCGAA CGUGUCACGUTT-3'), miR-466g inhibitor (5'-GTGTTG CGTGTATGTGTA-3') or miRNA inhibitor NC (5'-GTGTAA CACGTCTATACGCCCA-3' (Shanghai GenePharma Co., Ltd.) at a final concentration of 50 nM using Lipofectamine® 2000 reagent (Invitrogen; Thermo Fisher Scientific, Inc.) at 37˚C for 48 h. After 48 h, cells were used in subsequent experiments.

CCl_4 liver injury model. The present study was approved by the Animal Care and Use Committee of Tangdu Hospital of Air Force Medical University [approval no. TDYY(2019)033; Xi'an, China]. All experiments were performed in accordance with the approved National Institutes of Health Guidelines for the Care and Use of Laboratory Animals (20). C57BL/6 J male mice (n=12; 6 weeks old, 18-22 g) were obtained from the Institute of Laboratory Animal Sciences (Chinese Academy of Medical Sciences; Peking Union Medical College). The mice were maintained under the following conditions: 40-60% humidity at 18-23˚C, 12-h light-dark cycle (light on from 8:00 am to 8:00 pm) and with free access to food and water. Following acclimation for 1 week, a liver fibrosis mouse model was constructed via intraperitoneal injections of CCl_4 (7 μl/g body weight; Sigma-Aldrich; Merck KGaA) every week for 7 weeks, which was dissolved in corn oil. After 21 days, all mice were intraperitoneally euthanized with 3% sodium pentobarbital (160 mg/kg; Sigma-Aldrich; Merck KGaA) using a standard acceptable euthanasia method. Liver specimens and serum samples were obtained for analyses.

Histological analysis. Liver tissues were fixed with 10% buffered formalin at room temperature for 24 h and embedded in paraffin. Then, the sections (5-μm) were stained with Sirius Red at room temperature for 2 h (Sigma-Aldrich; Merck KGaA) and visualized under a light microscope (magnification, x200).

RT-qPCR. Total RNA was extracted from tissues and cells using TRIzol® reagent (Invitrogen; Thermo Fisher Scientific, Inc.). Total RNA was reverse-transcribed into cDNA using a PrimeScript™ RT-qPCR kit (Takara Bio, Inc.) according to the manufacturer's protocols at 37˚C for 75 min. qPCR was subsequently performed using SYBR Green mixture (Takara Bio, Inc.). The thermocycling conditions were as follows: 95˚C for 30 sec, followed by 40 cycles of 95˚C for 15 sec and 60˚C for 35 sec. Relative expression was calculated using the $2^{-\Delta\Delta Cq}$ method (21). Relative expression levels were normalized to the internal reference genes U6 or GAPDH. The primer sequences used were as follows: lnc-MBI-52 forward (F), 5'-GTCCAGGGACCTCTGACCTA-3' and reverse (R), 5'-CTGGAGAATCACCCCGACTG-3'; miR-466g F, 5'-CACTAGTGGTTCCGTTTAGTAG-3' and R, 5'-TTG TAGTCACTAGGGCACC-3'; α-SMA F, 5'-CACCATCGG GAATGAACGCTTC-3' and R, 5'-CTGTCAGCAATGCCT GGGTA-3'; Col-1 F, 5'-GGTCATTCTCTTCGCAGACAG-3' and R, 5'-CCACCGGATACTTGGTCTCCA-3'; SMAD4 F, 5'-CTCATGTGATCTATGCCCGTC-3' and R, 5'-AGG TGATACAACTCGTTCGTAGT-3'; U6 F, 5'-CTCGCTTCG GCAGCACA-3' and R, 5'-AACGCTTCACGAATTTGCGT-3; and GAPDH F, 5'-AAGGTGAAGGTCGGAGTCA-3' and R, 5'-GGAAGATGGTGATGGGATTT-3'.

Western blotting. Transfected HSCs cells were harvested after 48 h and lysed using RIPA lysis buffer (Sigma-Aldrich; Merck KGaA). Protein concentration was calculated using a BCA kit (Pierce; Thermo Fisher Scientific, Inc.). Protein (30 μg/lane) was separated via SDS-PAGE on a 12% gel, transferred onto PVDF membranes and subsequently blocked with 5% non-fat milk at room temperature for 80 min. The membranes were incubated overnight at 4˚C with primary antibodies (1:1,000) against Col-1 (cat. no. ab34710), α-SMA (cat. no. ab5694), SMAD4 (cat. no. ab40759) and GAPDH (cat. no. ab9485 (all purchased from Abcam). Following the primary antibody incubation, membranes were incubated with goat anti-rabbit antibody (cat. no. ab205718; 1:2,000; Abcam) at room temperature for 2 h. Protein bands were visualized using BeyoECL Plus (Beyotime Institute of Biotechnology).

CCK-8 assay. After transfection, cells were seeded into a 96-well plate (2x10^3 cells/well). Then, cells were collected and washed with PBS. After culture for 48 h, cells were incubated with 10 μl CCK solution at 37˚C for 2 h. The absorbance values were determined with a microplate reader at 450 nm.

Dual-luciferase reporter assay. The targets of lnc-MBI-52 and miR-466g were predicted using miRDB (http://mirdb.org) and TargetScan 7.2 (http://www.targetscan.org/vert_72). The

wild-type (WT) or mutant (MUT) sequences of the SMAD4 and lnc-MBI-52 prediction region were generated by PCR and cloned into the pGL3 luciferase reporter vector (Promega Corporation) located at *Kpn*I and *Bam*HI sites. The pGL3 vectors containing SMAD4 and lnc-MBI-52 WT or MUT predicted binding regions were co-transfected with the WT or MUT 3'-untranslated region of lnc-MBI-52 (or SMAD4) and miR-466g mimics or mimic NC into HSCs using Lipofectamine® 2000 reagent (Invitrogen; Thermo Fisher Scientific, Inc.) at 37˚C for 48 h. After 48 h, luciferase activity was detected via a dual-luciferase assay kit (Promega Corporation). Firefly luciferase activity was normalized to *Renilla* luciferase activity.

RNA pull-down assay. The biotin-labeled miR-466g and control probes were synthesized by Sangon Biotech Co., Ltd. The probes were co-incubated with streptavidin-coated microspheres (Invitrogen; Thermo Fisher Scientific, Inc.) at 25˚C for 2 h. HSCs were collected and lysed using Pierce IP lysis buffer (Thermo Fisher Scientific, Inc.). Cellular lysates (50 µl) were incubated with miR-466g or control probes overnight at 4˚C. The immunoprecipitate was obtained via magnetic forces and centrifugation at 1,000 x g for 20 min at room temperature, and then washed using the Pierce™ Magnetic RNA Pull-Down kit (Thermo Fisher Scientific, Inc.). 40 µl streptavidin magnetic beads were isolated from the supernatant after centrifugation (2,500 x g; 5 min; 4˚C) and washed with washing buffer (10 mM Tris-HCl pH 7.5, 1 mM EDTA, 2 M NaCl and 0.1% Tween-20), followed by another centrifugation step (2,500 x g; 5 min; 4˚C). The beads (100 µl; Sigma-Aldrich; Merck KGaA) were eluted and the complex was chilled on ice for 3 min before separating the beads and purification using TRIzol® reagent (Invitrogen; Thermo Fisher Scientific, Inc.). The results were detected using RT-qPCR as previously described. Proteins of the RNA-protein complexes were eluted from the magnetic beads by boiling (8 min at 100˚C), and SMAD4 protein expression was examined as aforementioned via western blotting using the antibody against SMAD4 (1:5,000).

Statistical analysis. All experiments were performed in triplicate. Data were analyzed using SPSS 22.0 software (IBM Corp.) and presented as the mean ± SEM. One-way ANOVA followed by Tukey's post hoc test were used to compare differences between multiple groups. P<0.05 was considered to indicate a statistically significant difference.

Results

lnc-MBI-52 is upregulated in liver fibrosis models in vivo and in vitro. To investigate the role of lnc-MBI-52 in liver fibrosis, its expression levels were detected both *in vivo* and *in vitro*. In the *in vivo* assay, CCl_4 increased the Sirius Red staining area (Fig. 1A). Moreover, the protein expression levels of α-SMA and Col-1 were increased, suggesting that the *in vivo* hepatic fibrosis model was successfully established (Fig. 1B). lnc-MBI-52 expression was significantly upregulated in liver fibrosis mice compared with the control group (P<0.01; Fig. 1C). This was consistent with the results of the *in vitro* assay. In addition, following treatment with TGF-β1, lnc-MBI-52 expression was significantly increased in HSCs compared with the control group (P<0.01; Fig. 1D).

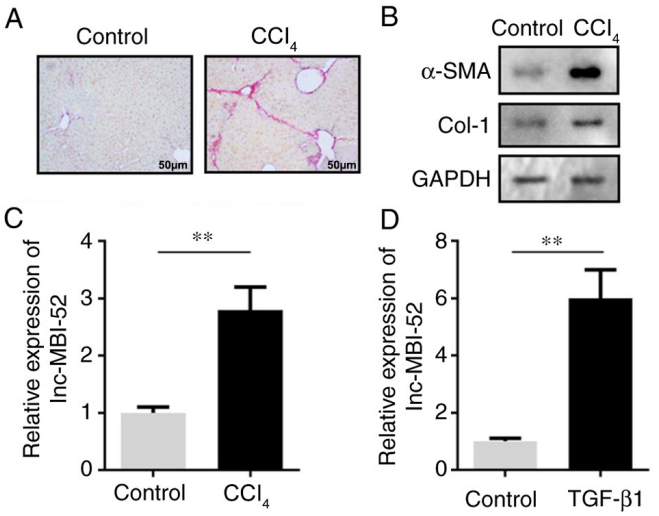

Figure 1. lnc-MBI-52 expression is upregulated during liver fibrosis. (A) Histological analysis of liver fibrosis was performed using Sirius Red staining. (B) The protein expression levels of α-SMA and Col-1 were detected by western blotting. (C) The expression of lnc-MBI-52 was upregulated in the CCl_4-induced hepatic fibrosis group compared with the control group. (D) The expression of lnc-MBI-52 was upregulated in LX-2 cells treated with TGF-β1. **P<0.01. lnc, long non-coding RNA; α-SMA, α-smooth muscle actin; Col-1, collagen type I; CCl_4, carbon tetrachloride.

Silencing lnc-MBI-52 alleviates liver fibrosis. To determine the role of lnc-MBI-52 in the progression of liver fibrosis, the expression of lnc-MBI-52 was suppressed with si-lnc-MBI-52. As presented in Fig. 2A, lnc-MBI-52 expression was significantly decreased by si-lnc-MBI-52 in cells, which was more potent in the si-lnc-MBI-52 1# group (P<0.05). Thus, si-lnc-MBI-52 1# was used in subsequent experiments. Cell viability was assessed, and the results demonstrated that following treatment with TGF-β1 viability of HSCs was increased compared with the control group (P<0.01). Furthermore, transfection with si-lnc-MBI-52 significantly decreased the viability of HSCs compared with the TGF-β1 + si-NC group (P<0.05; Fig. 2B). In addition, knockdown of lnc-MBI-52 inhibited α-SMA and Col-1 expression induced by the si-NC group (P<0.05; Fig. 2C-E). Taken together, these results suggested that lnc-MBI-52 knockdown could inhibit the progression of liver fibrosis.

Interaction between lnc-MBI-52 and miR-466g. lncRNAs modulate the expression of miRNAs by binding to their 3'-untranslated regions (22). Thus, the present study investigated the inhibitory effect of lnc-MBI-52 on miRNAs. miR-466g was predicted as a potential target of lnc-MBI-52 using miRDB (Fig. 3A). Furthermore, the results of the dual-luciferase reporter assay demonstrated that miR-466g mimics decreased the luciferase activity of pmirGLO-lnc-MBI-52-WT without affecting pmirGLO-lnc-MBI-52-MUT (P<0.01; Fig. 3B). To verify these results, miR-466g expression was assessed in HSCs transfected with si-lnc-MBI-52. lnc-MBI-52 expression was significantly upregulated by lnc-MBI-52 overexpression plasmids compared with the NC OE group (P<0.01; Fig. 3C).

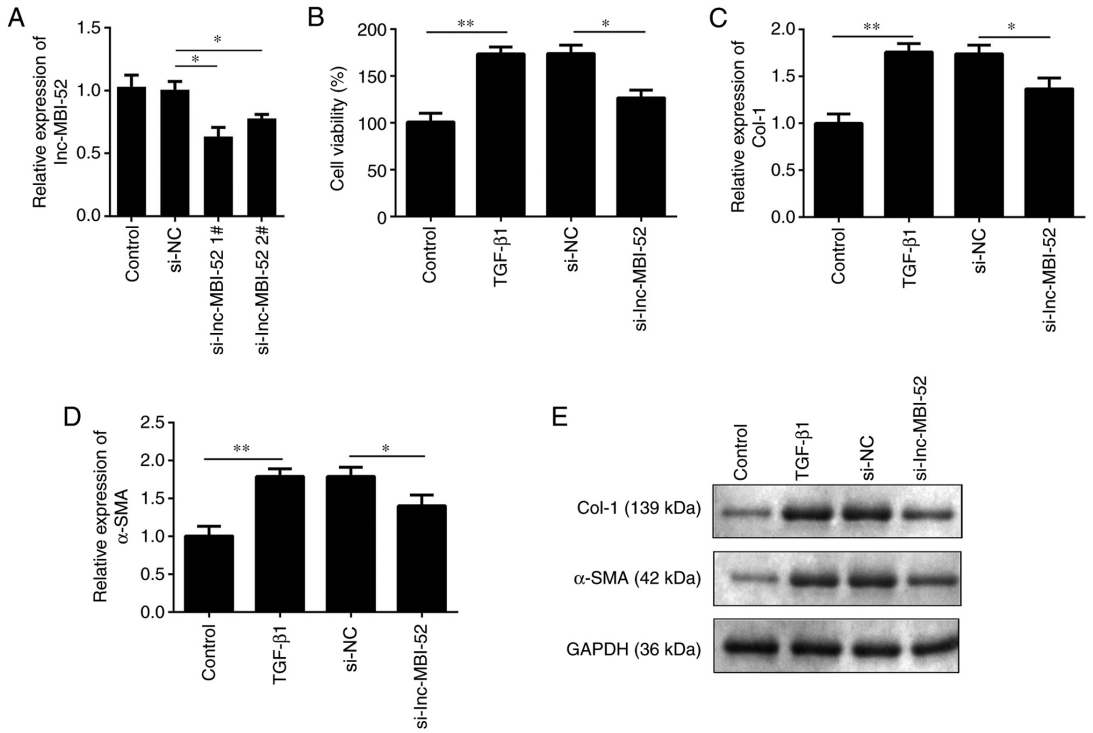

Figure 2. Knockdown of lnc-MBI-52 suppresses TGF-β1-induced liver fibrosis *in vitro*. (A) The expression of lnc-MBI-52 following transfection with si-lnc-MBI-52. (B) Cell viability determined using Cell Counting Kit-8 assay. The expression levels of (C) Col-1 and (D) α-SMA were detected via reverse transcription-quantitative PCR. (E) The protein expression levels of α-SMA and Col-1 were detected by western blotting. GAPDH was used as an internal control. *P<0.05, **P<0.01. lnc, long non-coding RNA; si-, small interfering RNA; α-SMA, α-smooth muscle actin; Col-1, collagen type I; NC, negative control.

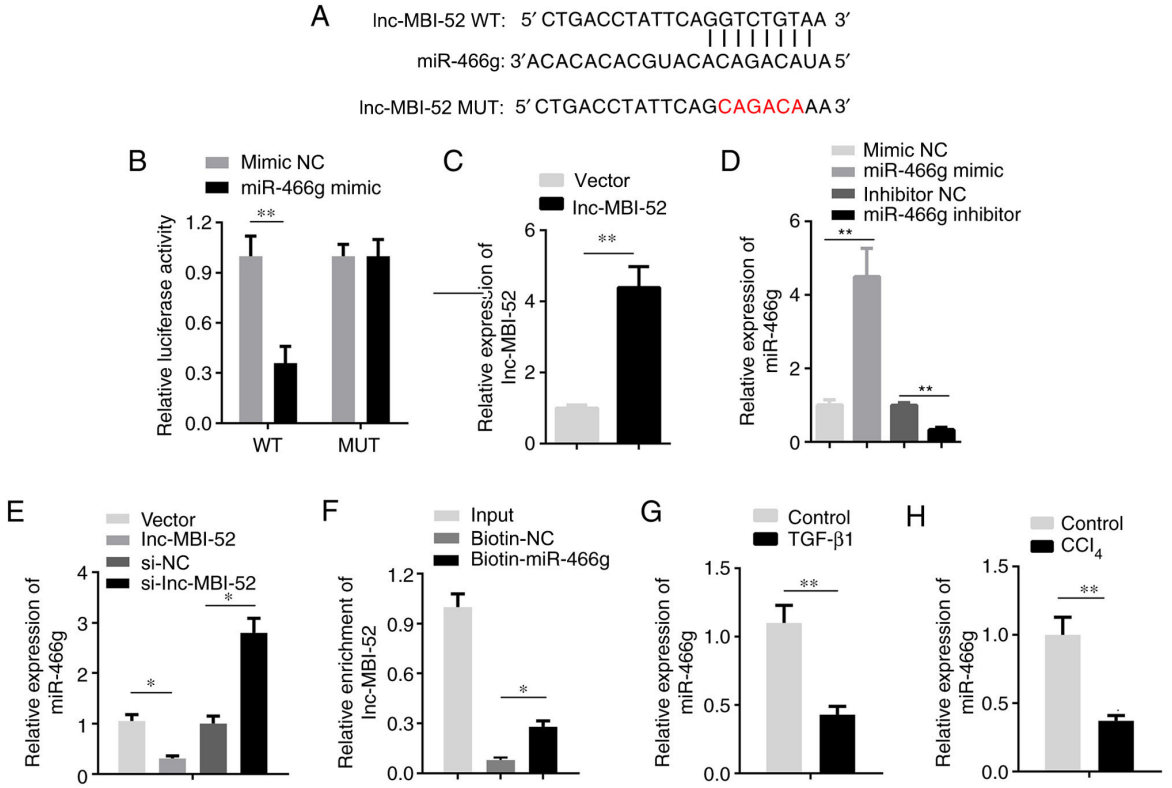

Figure 3. lnc-MBI-52 sponges miR-466g. (A) The binding sites between lnc-MBI-52 and miR-466g. (B) The interaction between lnc-MBI-52 and miR-466g was verified by dual-luciferase reporter assay. (C) The expression of lnc-MBI-52 was detected via RT-qPCR. (D) The transfection efficiency of miR-466g mimics and inhibitors detected via RT-qPCR. (E) lnc-MBI-52 negatively mediates miR-466g expression. (F) The interaction between lnc-MBI-52 and miR-466g was determined by RNA pull-down assay. (G) The expression of miR-466g was downregulated in LX-2 cells treated with TGF-β1. (H) The expression of miR-466g was downregulated in the CCl_4-induced hepatic fibrosis group compared with the control group. *P<0.05, **P<0.01. lnc, long non-coding RNA; si-, small interfering RNA; miR, microRNA; RT-qPCR, reverse transcription-quantitative PCR; NC, negative control; CCl_4, carbon tetrachloride; WT, wild-type; MUT, mutant; OE, overexpression.

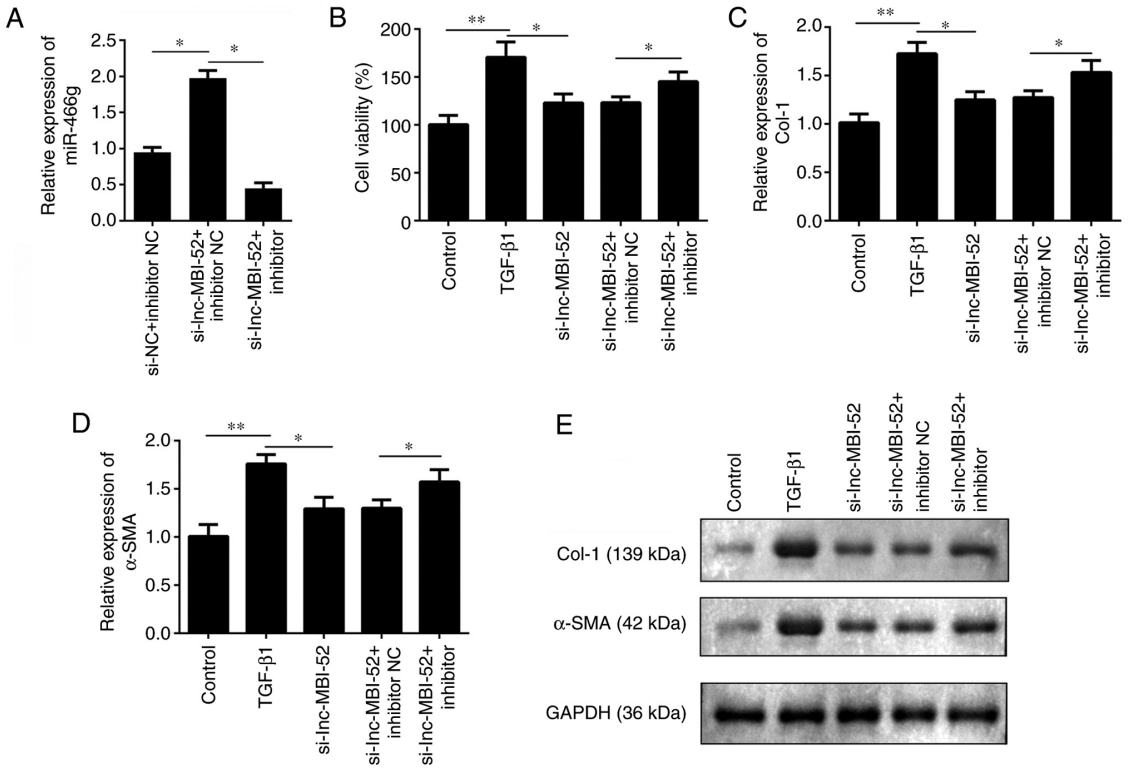

Figure 4. Knockdown of miR-466g alleviates the effects of lnc-MBI-52 knockdown on liver cell fibrosis. (A) The expression of miR-466g following transfection with si-lnc-MBI-52 or inhibitor treatment. (B) Cell viability was determined by a Cell Counting Kit-8 assay. The expression levels of (C) Col-1 and (D) α-SMA were detected via reverse transcription-quantitative PCR. (E) The protein expression levels of α-SMA and Col-1 were detected via western blotting. GAPDH was used as an internal control. *P<0.05, **P<0.01. lnc, long non-coding RNA; si-, small interfering RNA; miR, microRNA; α-SMA, α-smooth muscle actin; Col-1, collagen type I; NC, negative control.

The expression of miR-466g was significantly increased by transfection with the miR-466g mimic compared with the mimic NC group, and downregulated following transfection with the miR-466g inhibitor compared with the inhibitor NC group (P<0.01; Fig. 3D). The results demonstrated that lnc-MBI-52 overexpression vector significantly decreased miR-466g expression compared with the NC OE group (P<0.05; Fig. 3E). Conversely, miR-466g expression increased following transfection with si-lnc-MBI-52 compared with the si-NC group (P<0.05; Fig. 3E). The results of the RNA pull-down assay verified the interaction between lnc-MBI-52 and miR-466g (P<0.05; Fig. 3F). miR-466g expression was assessed in a mouse model of CCl_4-induced liver fibrosis and in HSCs treated with TGF-β1. The results demonstrated that miR-466g expression was significantly decreased in liver fibrosis models *in vivo* and *in vitro* (P<0.01; Fig. 3G and H).

Knockdown of lnc-MBI-52 inhibits liver fibrosis by interacting with miR-466g in vitro. A rescue experiment was performed to investigate the effect of miR-466g on liver fibrosis. As presented in Fig. 4A, cells were divided into three groups: si-NC + inhibitor NC, si-lnc-MBI-52 + inhibitor NC and si-lnc-MBI-52 + miR-466g inhibitor. si-lnc-MBI-52 significantly increased miR-466g expression compared with the si-NC + inhibitor NC group, which was alleviated by transfection with the miR-466g inhibitor (P<0.05). The viability of HSCs was subsequently assessed. After exposure to TGF-β1, cells were transfected with si-lnc-MBI-52 and/or miR-466g inhibitor or inhibitor NC. Compared with the TGF-β1 group, adding si-lnc-MBI-52 significantly decreased the viability of HSCs compared with TGF-β1 group (P<0.05); however, cell viability was partially restored following addition of miR-466g inhibitor (P<0.05; Fig. 4B). Furthermore, knockdown of miR-466g promoted the expression levels of α-SMA and Col-1 compared with the si-lnc-MBI-52 + inhibitor NC group (P<0.05; Fig. 4C-E). Collectively, these results suggested that the progression of liver fibrosis may be promoted by miR-466g knockdown.

miR-466g activates HSCs via the SMAD4 pathway. The TargetScan database was used to predict whether SMAD4 is a target of miR-466g. The target binding region between miR-466g and SMAD4 presented in Fig. 5A. In addition, the dual-luciferase reporter assay demonstrated that miR-466g mimics decreased the luciferase activity of pmirGLO-SMAD4-WT, without affecting pmirGLO-SMAD4-MUT (P<0.01; Fig. 5B). To verify these results, SMAD4 expression was assessed in HSCs transfected with miR-466g mimic or miR-466g inhibitor. The results demonstrated that transfection with the miR-466g mimic significantly decreased SMAD4 expression compared with the mimic NC group (P<0.05; Fig. 5C). Conversely, SMAD4 expression increased following transfection with the miR-466g inhibitor compared with the inhibitor NC group (P<0.05; Fig. 5C). In addition, SMAD4 protein expression increased following transfection with the miR-466g inhibitor, and decreased following transfection with the miR-466g mimic, compared with the corresponding NC groups (Fig. 5D).

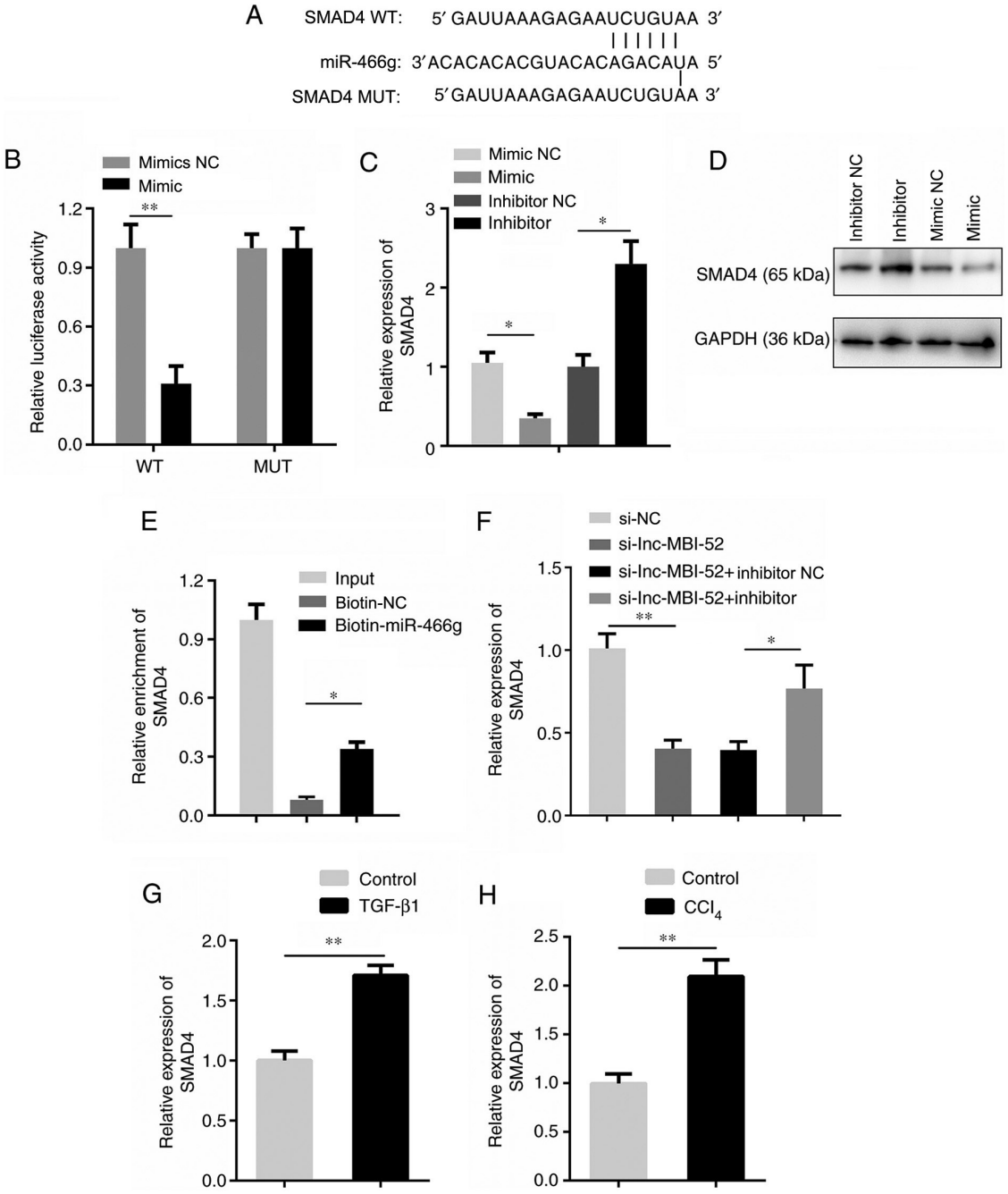

Figure 5. SMAD4 is a target of miR-466g. (A) The binding sites between miR-466g and SMAD4. (B) Luciferase activity was determined via dual-luciferase reporter assay. (C) SMAD4 was negatively regulated by miR-466g expression. (D) The protein expression of SMAD4 after miR-466g mimic or inhibitor treatment. (E) The interaction between SMAD4 and miR-466g was detected by RNA pull-down assay. (F) The expression of SMAD4 was determined via reverse transcription-quantitative PCR. (G) The expression of SMAD4 was upregulated in LX-2 cells treated with TGF-β1. (H) The expression of SMAD4 was upregulated in the CCl_4-induced hepatic fibrosis group. *P<0.05, **P<0.01. lnc, long non-coding RNA; si-, small interfering RNA; miR, microRNA; NC, negative control; CCl_4, carbon tetrachloride; WT, wild-type; MUT, mutant; OE, overexpression.

The RNA pull-down assay verified the interaction between SMAD4 and miR-466g (P<0.05; Fig. 5E). The expression of SMAD4 was significantly decreased by lnc-MBI-52 knockdown compared with the si-NC group (P<0.01), which was partially restored by transfection with the miR-466g inhibitor (P<0.05; Fig. 5F). SMAD4 expression was assessed in mice with CCl_4-induced liver fibrosis and HSCs treated with TGF-β1. The results demonstrated that SMAD4 expression was significantly upregulated in liver fibrosis both *in vivo* and *in vitro* (P<0.01; Fig. 5G and H).

Discussion

Liver fibrosis increases the incidence of cirrhosis (23). Inhibiting the proliferation of HSCs and promoting collagen degradation has been reported as an effective means for treating liver fibrosis (24). Thus, understanding the molecular mechanism underlying HSC activation may provide novel insights into the development of more effective strategies to decrease the incidence of liver fibrosis. lnc-MBI-52 is a newly discovered lncRNA. The results of the present study demonstrated

that lnc-MBI-52 expression increased during the process of liver fibrosis, both *in vivo* and *in vitro*. In addition, following lnc-MBI-52 knockdown, the expression levels of α-SMA and Col-1 were significantly decreased. Moreover, lnc-MBI-52 was observed to promote liver fibrosis via the miR-466g/SAMD4 axis. To the best of our knowledge, the present study was the first to demonstrate that lnc-MBI-52 plays a role in promoting liver fibrosis.

lncRNAs play crucial roles in the development of liver fibrosis, whereby alterations in their expression levels and mutations may promote or inhibit the occurrence of liver fibrosis (25-27). It was previously demonstrated that lnc-LFAR1 directly binds to SMAD2/3 and promotes TGF-β and Notch pathway activation, which in turn activates HSCs and promotes liver fibrosis (14). In addition, lnc-H19 can promote the progression of cholestatic liver fibrosis, mainly by promoting HSC differentiation and activation (28). Shen *et al* (29) reported that the MAPK signaling pathway could be inhibited by silencing lncRNA HULC to reverse liver fibrosis in non-alcoholic fatty liver disease *in vivo* and decrease hepatocyte apoptosis. The results of the present study demonstrated that lnc-MBI-52 expression was increased in liver fibrosis models, both *in vivo* and *in vitro*. However, lnc-MBI-52 knockdown inhibited the activation of HSCs and promoted α-SMA and Col-1 degradation, which may affect the occurrence and development of liver fibrosis (30). Thus, knockdown of lnc-MBI-52 may protect against liver fibrosis. However, the underlying molecular mechanisms remain unclear.

A number of studies have confirmed that lncRNAs act as molecular sponges to regulate miRNA expression and biological functions (31,32). miRNAs play key roles in the occurrence and progression of liver fibrosis (33-35). A previous study reported that miR-122 plays an inhibitory role in liver fibrosis by inhibiting the activation of HSCs and the expression of fibrosis-related genes (36). Another study demonstrated that exosomes derived from adipose mesenchymal stem cells modified with miR-181-5p prevent liver fibrosis via autophagy activation (18). miRNAs are highly conserved RNAs that exhibit a high degree of homology between different species. Jia *et al* (37) demonstrated that miR-466 inhibits the aggressive behavior of hepatocellular carcinoma by directly targeting metadherin. However, the results of the present study demonstrated that knockdown of miR-466g reversed the activation of HSCs and the downregulation of α-SMA and Col-1 expression induced by lnc-MBI-52 knockdown. Thus, lnc-MBI-52 may participate in the development of liver fibrosis by inhibiting miR-466g expression.

Accumulating evidence suggests that miRNAs interact with their targets to participate in the development of liver fibrosis (33,38). In the present study, SMAD4 was predicted and proven to be a target of miR-466g. SMAD4 regulates a considerable number of fundamental cellular processes, such as protein synthesis and cell proliferation (39). For example, SMAD4 interacts with SMAD2/3 in cells and participates in mediating the effects of the TGF-β signaling pathway (40). It has been demonstrated that overexpression of miR-34 in HSCs can reverse the development of liver fibrosis by targeting SMAD4 (19). A previous study demonstrated that, following SMAD4 gene knockout, liver fibrosis in mice significantly decreased, suggesting that SMAD4 knockdown can delay the progression of liver fibrosis (41). SMAD4 plays key roles in fibrotic diseases; thus, inhibition of SMAD4 may decrease fibrosis by decreasing the activity of the SMAD3 responsive promoter. The results of the present study demonstrated that downregulation of SMAD4 inhibited the activation of HSCs and the expression levels of α-SMA and Col-1, and that miR-466g may participate in the development of liver fibrosis by inhibiting SMAD4 expression.

However, there are limitations in this study. This study mainly focused on the competing endogenous RNA potential of lnc-MBI-52. However, lncRNAs may interact with RNA binding proteins to regulate gene expression and biological processes, which requires further study. Further studies will use clinical samples to verify the potentials of lnc-MBI-52 in liver fibrosis.

In conclusion, the results presented herein indicated the role of the lnc-MBI-52/miR-466g/SMAD4 signaling cascade in liver fibrosis and further highlighted the promoting effect of lnc-MBI-52 in this disease.

Acknowledgements

Not applicable.

Funding

No funding was received.

Availability of data and materials

The datasets used and/or analyzed during the current study are available from the corresponding author on reasonable request.

Authors' contributions

YL drafted the manuscript and worked with PL to perform the experiments, collect the data and interpret the data. FW conceived and designed the study and revised the manuscript. PL and FW confirm the authenticity of all the raw data. All authors have read and approved the final manuscript.

Ethics approval and consent to participate

The present study was approved by the Animal Care and Use Committee of Tangdu Hospital of Air Force Medical University [approval no. TDYY(2019)033; Xi'an, China]. All experiments were performed in accordance with the approved National Institutes of Health Guidelines for the Care and Use of Laboratory Animals.

Patient consent for publication

Not applicable.

Competing interests

The authors declare that they have no competing interests.

References

1. Aydin MM and Akcali KC: Liver fibrosis. Turk J Gastroenterol 29: 14-21, 2018.
2. Hernandez-Gea V and Friedman SL: Pathogenesis of liver fibrosis. Annu Rev Pathol 6: 425-456, 2011.
3. Parola M and Pinzani M: Liver fibrosis: Pathophysiology, pathogenetic targets and clinical issues. Mol Aspects Med 65: 37-55, 2019.
4. Sun M and Kisseleva T: Reversibility of liver fibrosis. Clin Res Hepatol Gastroenterol 39 (Suppl 1): S60-S63, 2015.
5. Jarroux J, Morillon A and Pinskaya M: History, discovery, and classification of lncRNAs. Adv Exp Med Biol 1008: 1-46, 2017.
6. Robinson EK, Covarrubias S and Carpenter S: The how and why of lncRNA function: An innate immune perspective. Biochim Biophys Acta Gene Regul Mech 1863: 194419, 2020.
7. Jathar S, Kumar V, Srivastava J and Tripathi V: Technological developments in lncRNA biology. Adv Exp Med Biol 1008: 283-323, 2017.
8. Zhu J, Fu H, Wu Y and Zheng X: Function of lncRNAs and approaches to lncRNA-protein interactions. Sci China Life Sci 56: 876-885, 2013.
9. Murillo-Maldonado JM and Riesgo-Escovar JR: The various and shared roles of lncRNAs during development. Dev Dyn 248: 1059-1069, 2019.
10. Bhan A, Soleimani M and Mandal SS: Long noncoding RNA and cancer: A new paradigm. Cancer Res 77: 3965-3981, 2017.
11. Bian EB, Xiong ZG and Li J: New advances of lncRNAs in liver fibrosis, with specific focus on lncRNA-miRNA interactions. J Cell Physiol 234: 2194-2203, 2019.
12. He Z, Yang D, Fan X, Zhang M, Li Y, Gu X and Yang M: The roles and mechanisms of lncRNAs in liver fibrosis. Int J Mol Sci 21: 1482, 2020.
13. Hanson A, Wilhelmsen D and DiStefano JK: The role of long non-coding RNAs (lncRNAs) in the development and progression of fibrosis associated with nonalcoholic fatty liver disease (NAFLD). Noncoding RNA 4: 18, 2018.
14. Zhang K, Han X, Zhang Z, Zheng L, Hu Z, Yao Q, Cui H, Shu G, Si M, Li C, *et al*: The liver-enriched lnc-LFAR1 promotes liver fibrosis by activating TGFβ and Notch pathways. Nat Commun 8: 144, 2017.
15. Zhang K, Han Y, Hu Z, Zhang Z, Shao S, Yao Q, Zheng L, Wang J, Han X, Zhang Y, *et al*: SCARNA10, a nuclear-retained long non-coding RNA, promotes liver fibrosis and serves as a potential biomarker. Theranostics 9: 3622-3638, 2019.
16. Zhao Z, Lin CY and Cheng K: siRNA- and miRNA-based therapeutics for liver fibrosis. Transl Res 214: 17-29, 2019.
17. Lan T, Li C, Yang G, Sun Y, Zhuang L, Ou Y, Li H, Wang G, Kisseleva T, Brenner D and Guo J: Sphingosine kinase 1 promotes liver fibrosis by preventing miR-19b-3p-mediated inhibition of CCR2. Hepatology 68: 1070-1086, 2018.
18. Qu Y, Zhang Q, Cai X, Li F, Ma Z, Xu M and Lu L: Exosomes derived from miR-181-5p-modified adipose-derived mesenchymal stem cells prevent liver fibrosis via autophagy activation. J Cell Mol Med 21: 2491-2502, 2017.
19. Feili X, Wu S, Ye W, Tu J and Lou L: MicroRNA-34a-5p inhibits liver fibrosis by regulating TGF-β1/Smad3 pathway in hepatic stellate cells. Cell Biol Int 42: 1370-1376, 2018.
20. Petersen BW, Harms TJ, Reynolds MG and Harrison LH: Use of vaccinia virus smallpox vaccine in laboratory and health care personnel at risk for occupational exposure to orthopoxviruses-recommendations of the advisory committee on immunization practices (ACIP), 2015. MMWR Morb Mortal Wkly Rep 65: 257-262, 2016.
21. Livak KJ and Schmittgen TD: Analysis of relative gene expression data using real-time quantitative PCR and the 2(-Delta Delta C(T)) method. Methods 25: 402-408, 2001.
22. Khatun M, Sur S, Steele R, Ray R and Ray RB: Inhibition of long noncoding RNA linc-pint by hepatitis C virus in infected hepatocytes enhances lipogenesis. Hepatology 74: 41-54, 2021.
23. Campana L and Iredale JP: Regression of liver fibrosis. Semin Liver Dis 37: 1-10, 2017.
24. Zhang CY, Yuan WG, He P, Lei JH and Wang CX: Liver fibrosis and hepatic stellate cells: Etiology, pathological hallmarks and therapeutic targets. World J Gastroenterol 22: 10512-10522, 2016.
25. Xiao Y, Liu R, Li X, Gurley EC, Hylemon PB, Lu Y, Zhou H and Cai W: Long noncoding RNA H19 contributes to cholangiocyte proliferation and cholestatic liver fibrosis in biliary atresia. Hepatology 70: 1658-1673, 2019.
26. Peng H, Wan LY, Liang JJ, Zhang YQ, Ai WB and Wu JF: The roles of lncRNA in hepatic fibrosis. Cell Biosci 8: 63, 2018.
27. Chen MJ, Wang XG, Sun ZX and Liu XC: Diagnostic value of LncRNA-MEG3 as a serum biomarker in patients with hepatitis B complicated with liver fibrosis. Eur Rev Med Pharmacol Sci 23: 4360-4367, 2019.
28. Liu R, Li X, Zhu W, Wang Y, Zhao D, Wang X, Gurley EC, Liang G, Chen W, Lai G, *et al*: Cholangiocyte-derived exosomal long noncoding RNA H19 promotes hepatic stellate cell activation and cholestatic liver fibrosis. Hepatology 70: 1317-1335, 2019.
29. Shen X, Guo H, Xu J and Wang J: Inhibition of lncRNA HULC improves hepatic fibrosis and hepatocyte apoptosis by inhibiting the MAPK signaling pathway in rats with nonalcoholic fatty liver disease. J Cell Physiol 234: 18169-18179, 2019.
30. Feng J, Wang C, Liu T, Li J, Wu L, Yu Q, Li S, Zhou Y, Zhang J, Chen J, *et al*: Procyanidin B2 inhibits the activation of hepatic stellate cells and angiogenesis via the Hedgehog pathway during liver fibrosis. J Cell Mol Med 23: 6479-6493, 2019.
31. Huang Y: The novel regulatory role of lncRNA-miRNA-mRNA axis in cardiovascular diseases. J Cell Mol Med 22: 5768-5775, 2018.
32. Chen L, Zhou Y and Li H: LncRNA, miRNA and lncRNA-miRNA interaction in viral infection. Virus Res 257: 25-32, 2018.
33. Tsay HC, Yuan Q, Balakrishnan A, Kaiser M, Mobus S, Kozdrowska E, Farid M, Tegtmeyer PK, Borst K, Vondran FWR, *et al*: Hepatocyte-specific suppression of microRNA-221-3p mitigates liver fibrosis. J Hepatol 70: 722-734, 2019.
34. Caviglia JM, Yan J, Jang MK, Gwak GY, Affo S, Yu L, Olinga P, Friedman RA, Chen X and Schwabe RF: MicroRNA-21 and Dicer are dispensable for hepatic stellate cell activation and the development of liver fibrosis. Hepatology 67: 2414-2429, 2018.
35. Calvente CJ, Tameda M, Johnson CD, Del Pilar H, Lin YC, Adronikou N, De Mollerat Du Jeu X, Llorente C, Boyer J and Feldstein AE: Neutrophils contribute to spontaneous resolution of liver inflammation and fibrosis via microRNA-223. J Clin Invest 129: 4091-4109, 2019.
36. Zeng C, Wang YL, Xie C, Sang Y, Li TJ, Zhang M, Wang R, Zhang Q, Zheng L and Zhuang SM: Identification of a novel TGF-β-miR-122-fibronectin 1/serum response factor signaling cascade and its implication in hepatic fibrogenesis. Oncotarget 6: 12224-12233, 2015.
37. Jia C, Tang D, Sun C, Yao L, Li F, Hu Y, Zhang X and Wu D: MicroRNA466 inhibits the aggressive behaviors of hepatocellular carcinoma by directly targeting metadherin. Oncol Rep 40: 3890-3898, 2018.
38. Abdel-Al A, El-Ahwany E, Zoheiry M, Hassan M, Ouf A, Abu-Taleb H, Abdel Rahim A, El-Talkawy MD and Zada S: miRNA-221 and miRNA-222 are promising biomarkers for progression of liver fibrosis in HCV Egyptian patients. Virus Res 253: 135-139, 2018.
39. McCarthy AJ and Chetty R: Smad4/DPC4. J Clin Pathol 71: 661-664, 2018.
40. Zhao M, Mishra L and Deng CX: The role of TGF-β/SMAD4 signaling in cancer. Int J Biol Sci 14: 111-123, 2018.
41. Xu XB, He ZP, Leng XS, Liang ZQ, Peng JR, Zhang HY, Zhang HY, Xiao M, Zhang H, Liu CL and Zhang XD: Effects of Smad4 on liver fibrosis and hepatocarcinogenesis in mice treated with CCl4/ethanol. Zhonghua Gan Zang Bing Za Zhi 18: 119-123, 2010 (In Chinese).